Soil Water Dynamics Studies Using Image Analysis

Guillermo González Cervantes, Ignacio Sánchez-Cohen, Jean Pierre Rossignol

Abstract

Image analysis has become a powerful tool for describing soil porous media properties with hydrological purposes. In this study an experimental watershed in Northern Mexico was selected in order to characterize soil macro porosity and its variations in the soil profile for explaining runoff events. Preferential flow was determined using a colorant and then pore size and continuity was determined by means of image analysis. Four criteria were used for performing morphologic parameterization of pores: total porosity, pore size, pore shape and continuity and saturated hydraulic conductivity. Results have shown that horizons with low permeability have small pore size (<0.53 mm^2) and are rounded that function individually. On the other hand, horizons with higher permeability have both median size pores (form 0.53 to 1.58 mm^2) and big pores (>1.58 mm^2). The shape of these pores are enlarged and irregular with good continuity among them.

Keywords: soil pores, porosity, image analysis

Introduction

Distribution of water in soils takes place through void spaces (pores); in this way, organization and distribution of pores are of crucial importance for the transport and retention of water in the soil. This water it is used for crops evapotranspiration and or feeding aquifers. Also saturated hydraulic conductivity depends on the relative abundance and spatial distribution of void spaces. Volumetric description of soil porosity generally is not enough for explaining soil water dynamics (Hallaire et al. 1997). Therefore, soil porosity characterization based on the path of preferential water movement may be described and quantified based on three morphological criteria: a) size, b) shape and c) continuity. This may be pursued using image and analysis techniques which is a procedure that accounts for an important development in the study of soil porosity (Bouma et al. 1979; Stengel 1979, German and Beven 1981, Bullock and Mc Keague, 1984, Bruand 1986, Curmi, 1988, Grimaldi and Boulet 1989-90, Hallaire, 1997, Hallaire et al. 1997, González, 2002).

Objective

The overall objective of this study has been to describe soil porosity and the path of preferential soil water flux using image analysis through previously marked paths with a colorant (blue of methylene) over the main soil horizons in a watershed in northern Mexico.

Materials and Methods

Field work was carried out during 1999 in a watershed in northern Mexico known as Carboneras within the boundaries of the ranch Atotonilco located between parallels 24°33’ and 24°50’ north latitude, and the meridians 103°34’ and 103°50’ west longitude. Since a geological stand point Carboneras watershed is located over eruptive and sedimentary soil materials. Rocks and eruptive material are mainly located in the south part in the form of eruptive relieves and basaltic materials. Sedimentary materials are located due north in the form of dendrites materials of conglomerated and some calcareous materials (Figure 1).

González Cervantes and Sánchez-Cohen are Researchers, INIFAP - CENID RASPA, Durango, Mexico. E-mail: gonzalez@raspa.inifap.conacyt.mx. Jean Pierre Rossignol is a Maitre de Conferences, National Institute of Horticulture, Angers, France.

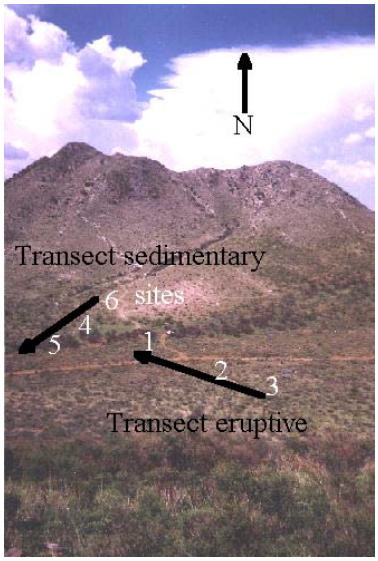

Figure 1. Carboneras Watershed and experimental sites.

Selection of representative soil horizons

After the soil description, six representative sites were selected in two transects as shown on Figure 1 (Gonzalez, 2002). These horizons are described in Figure 2.

Non disturbed soil monoliths of 1000 cm^3 were obtained using the Vergiere method (Bourier 1965). Saturated soil water conductivity (Ksat) was measured in the laboratory using a constant head infiltrometer (Beaudet 1998) and soil samples were obtained in order to determine physical and chemical characteristics (Table 1).

Soil paths characterization

Soil monoliths were saturated using a colorant blue of methylene ($C_{16}H_{18}CIN_{35}2H_20$) in a concentration of 1 $gr.l^{-1}$ during eight hours in order to highlight the pores that ensures preferential water flow in the soil (Bouma et al. 1979, Hallaire and Curmi 1994, Gonzalez 2002). Then the monoliths were saturated with acetone and impregnated with a polyester resin (Scott-Bader Crystic) containing a fluorescent pigment (Uvitex), (Murphy et al. 1977). Then horizontal thin layers of soil were obtained of approximately 3 cm in width.

Image analysis

Soil image analysis were performed using a camera (JVC 3CCD KY-F30B) with a data logger under the form of a rectangular matrix of 58 by 45 mm with a spatial resolution of 90µm by pixel highlighting soil samples by means of ultraviolet light for describing total porosity (Figure 3). Then using visible light for making evident marked paths with blue of methylene, image analysis was carried out using a special computer program (Optimas v5.2).

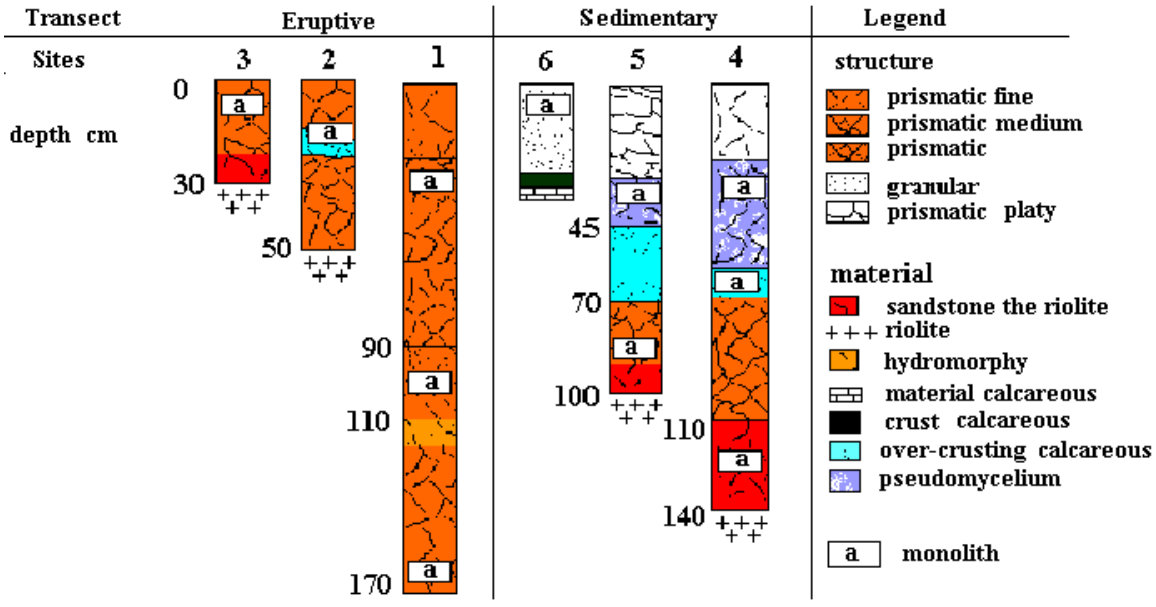

Figure 2. Site description of soil horizons.

Table 1. Physical and chemical characteristics of representative soil horizons of the eruptive and sedimentary transects.

Site	Depth	Clay	Silt %		Sand %		Carbon	pH water	Carbonate
	cm	%	fine	thick	fine	thick	Total	2/1	total %
3	15	22	4	11	40	23	1.5	7.7	0
2	15	18	16	12	37	17	1	7.4	0
	45	16	11	15	38	20	0.7	7.2	0
1	35	20	3	9	41	27	0.6	7.1	0
	115	7	27	12	34	20	0.3	7.5	0
6	5	14	16	13	34	23	6	8.2	34
5	15	17	16	12	28	27	3	8.1	9
	60	24	14	25	26	25	4	8.3	29
	95	18	21	12	25	24	0.6	8.4	3
4	10	12	25	12	26	25	2	8	1
	40	18	24	14	22	22	1	8	1
	65	26	18	14	20	22	2	8.3	15

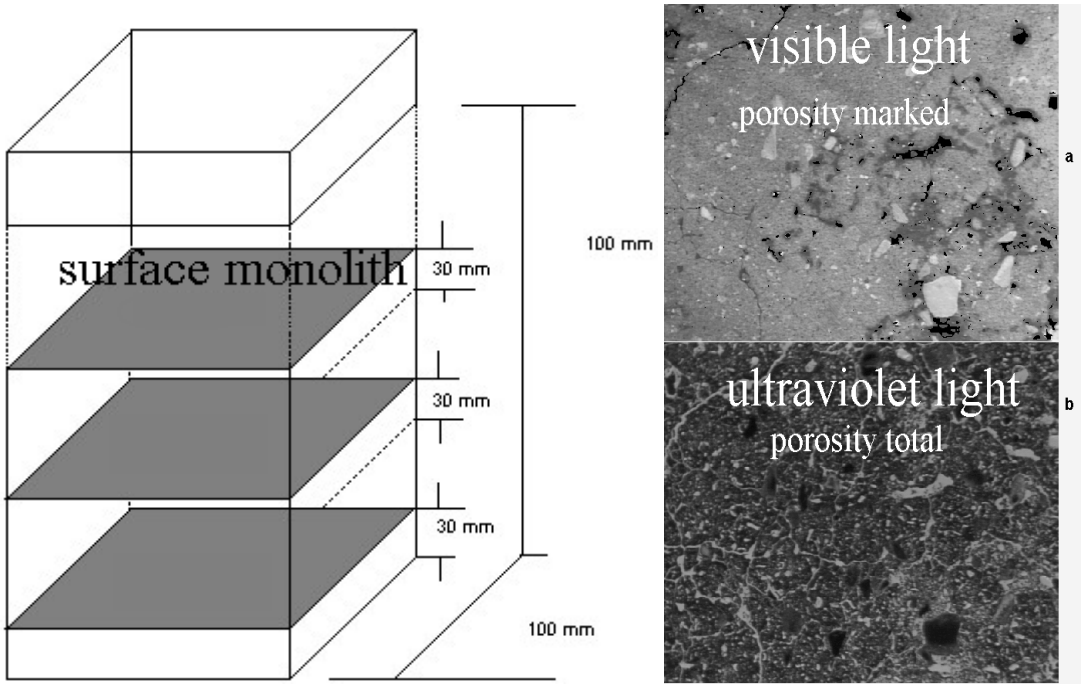

Figure 3. Monolith cutting and image sample.

Pores characteristics

Three morphologic parameters were used for characterizing soil pores. Pore size is computed using equation 1 which then was grouped in three different classes; T1 (small pores), T2 (medium sized pores) and T3 (big pores):

$$T = \frac{P^2}{4\pi x A} \quad (1)$$

where T is size pores, and P is perimeter (cm) and A is pore area (cm^2).

Pore shape is expressed by an enlargement index (Ia) grouping three classes: F1 (round pores), F2 (enlarged pores) and F3 (irregular pores); see Table 2.

Table 2. Soil pore classification according shape and size.

Pore Shape		**Pore Size**		
		T1 small	**T2 medium**	**T3 big**
		area < 0.53 mm²	**0.53< area < 1.58 mm²**	**area >1.58 mm²**
F1 round	Ia < 5	T1F1	T2F1	T3F1
F2 enlarged	5 < Ia < 10	T1F2	T2F2	T3F2
F3 irregular	Ia >10	T1F3	T2F3	T3F3

Continuity index is described by equation 2 (Serra 1982):

$$Ic = \frac{1 - Nc}{Un} \quad (2)$$

were *Ic* represent image pore continuity and variates from 0 to 1; *Nc* is the number of convex voids and *Un* is the number of concave voids. *Ic* is small when pores are isolated and increases when pores are ordered in a series.

Results

Figure 4 shows results of saturated hydraulic conductivity (Ksat) for the two transects. Ksat variates from 252 to 108 mm hr^{-1} for the eruptive transect and from 144 to 28.8 mm hr^{-1} for the sedimentary transect. Based on this, three groups may be distinguished: horizons with high Ksat, sites 3, 2 and 1 of the eruptive transect; site 6 of the sedimentary transect and horizons with low Ksat of sites 5 and 4 of the sedimentary transect.

These Ksat variations lead to describe and characterize soil porosity using image analysis and then to correlate Ksat with morphological characteristics of soil pores considering the type of calcareous accumulation for the sedimentary transect and the sandy materials from reolite alterations for the eruptive transect.

Total visible porosity at 90 µm

Tables 3 and 4 shows distribution of total visible average of porosity at 90µm as a function of size (T1 to T3) and shape (F1 to F3) for surface horizons.

In eruptive transect (Table 3) a soil porosity variation from 6.2 to 8.4 % was observed for surface horizons (site 3, 2 and 1) and from 8.4 to 13.4% for deeper horizons (site 1). This porosity is mainly formed by small pores (T1 < 0.53 mm^2) and in less proportion by medium sized pores (T2 from 0.53 to 1.58 mm^2) and big pores (T3 > 1.58 mm^2). This former category has a different and irregular enlarged pore distribution. Calcareous accumulation en site 2 prevent soil porosity analysis.

On the sedimentary transect (Table 4) total soil porosity ranged from 8.1 to 10.4 % for surface horizons (sites 6, 5 and 4) and from 9.2 to 12.2 % for deeper horizons (sites 5 and 4). Soils in this transect are characterized by having a calcareous accumulation in the form of a crust at different depths.

Soil porosity analysis allows to describe pores distribution. Nevertheless, results interpretation does not allows to differentiate soil horizons with and without calcareous formation. On the other hand, results confirm that Ksat does not depend on the soil porosity only.

From there, the necessity of analyzing soil pores continuity index by means of equation 2.

Soil pores continuity index (*Ic*)

Table 5 shows values of porous media continuity index (*Ic*) for both eruptive and sedimentary transects. Horizons with calcareous crust formation (sites 2 and 6), with encrustment (sit 4 at 65 cm depth) and pseudo micelle (site 5 at 15 cm depth and site 4 at 25 cm depth) shows *Ic* values lower that sites with riolite - sand particles (sites 3, 1 and 4 at 130 cm). This result allows to differentiate horizons with and without calcareous formations and highlight the importance of pore continuity. Next a description of functional porous space is proposed.

Functional porosity

Table 6 shows the percentage of soil pores marked wit blue of methylene for the eruptive transect. Functional porosity ranges from 0.35 to 2.2% for surface horizons.

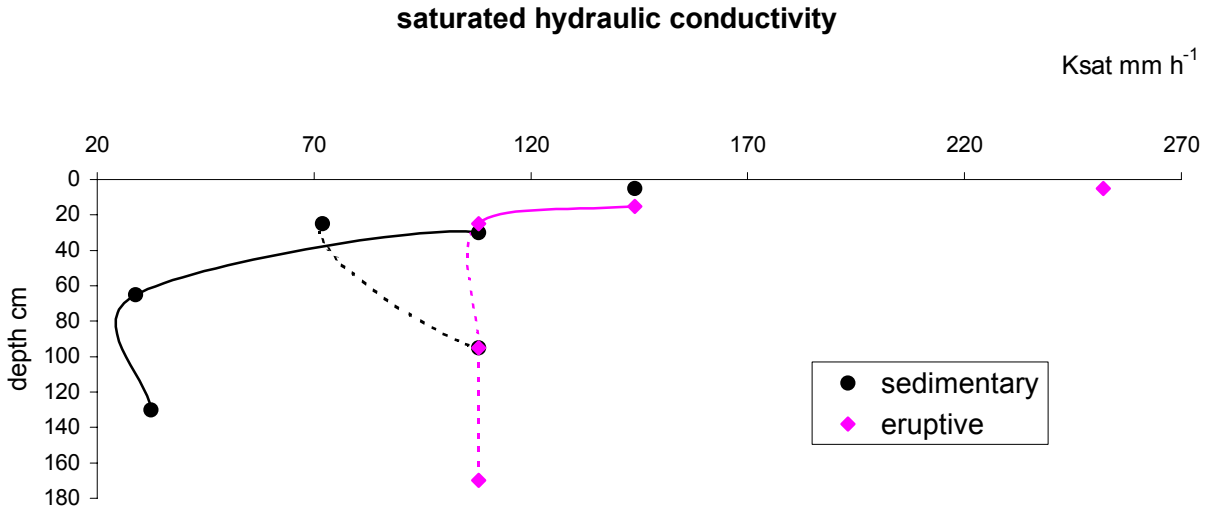

Figure 4. Values of saturated hydraulic conductivity (Ksat).

Table 3. Soil porosity characterization in the eruptive transect.

	Site 3			Site 2				Site 1			
pore	**T1**	**T2**	**T3**	**T1**	**T2**	**T3**	**depth cm**	**T1**	**T2**	**T3**	**depth cm**
round	2.9	0.4	0.3	3.5	0.1	0	15	5.5	0.5	0	25
enlarged	0.3	0.6	0.2	1.4	0.3	0.2		0.5	0.6	0.1	
irregular	0	0.2	1.3	0.4	0.9	1.3		0	0.2	1	
		total %	**6.2**			**8.1**				**8.4**	
							round	5.6	1.2	0.1	95
							enlarged	0.5	1.1	0.2	
							irregular	0	0.2	2.1	
									total %	**11**	
							round	6.2	1.7	0.5	170
							enlarged	0.5	1.2	0.9	
							irregular	0	0.2	2.2	
									total %	**13.4**	

Table 4. Soil porosity characterization in the sedimentary transect.

	Site 6				Site 5				Site 4			
pore	**T1**	**T2**	**T3**	**depth cm**	**T1**	**T2**	**T3**	**depth cm**	**T1**	**T2**	**T3**	**depth cm**
round	3.5	0.1	0	5	3.8	0.3	0.1	15	5.3	1	0.9	25
enlarged	1.4	0.3	0.2		1	0.9	0.1		0.4	1.1	1.2	
irregular	0.4	0.9	1.3		0.1	0.9	2		0	0.2	0.3	
		total %	**8.1**				**9.2**				**10.4**	
				round	5.4	0.5	0	95	5.4	0.5	0.2	65
				enlarged	1	0.7	0.2		0.6	0.6	0.3	
				irregular	0.1	0.4	0.4		0	0.2	0.5	
						total %	**8.7**				**8.3**	
								round	5	1.8	0.5	120
								enlarged	0.4	1.1	1.2	
								irregular	0	0.2	2	
										total %	**12.2**	

Table 5. Porous media continuity index (*Ic*).

Eruptive Transect			**Sedimentary Transect**		
site	**depth**	**Ic**	**site**	**depth**	**Ic**
3	5	0.32	6	5	0.06
2	15	0.04	5	30	0.03
				100	0.04
1	25	0.07	4	25	0.1
	95	0.1		65	0.06
	170	0.1		130	0.11

Table 6. Characterization of soil porosity in the eruptive transect marked with blue methylene.

	Site 3			Site 2				Site 1			
pore	**T1**	**T2**	**T3**	**T1**	**T2**	**T3**		**T1**	**T2**	**T3**	**depth**
round	0.9	0.1	0.3	0.2	0	0		0.4	0	0	25
enlarged	0.1	0.1	0.1	0.1	0.02	0		0	0.1	0	
irregular	0	0	0.6	0.03	0	0		0	0	0.4	
		pF %	**2.2**			**0.35**				**1.2**	
		p T %	**6.2**			**8.1**				**8.4**	
							round	2.7	0.6	0	95
							enlarged	0.2	0.6	0.1	
							irregular	0	0	1.1	
									pF %	**5.3**	
									p T %	**11**	
							round	2.1	0.7	0	170
							enlarged	0.2	0.7	0.3	
							irregular	0	0.1	2.1	
									pF %	**6.2**	
									p T %	**13.4**	

Table 7: Characterization of soil porosity in the sedimentary transect marked with blue methylene.

	Site 6				Site 5				Site 4			
pore	**T1**	**T2**	**T3**		**T1**	**T2**	**T3**	**depth cm**	**T1**	**T2**	**T3**	**depth cm**
round	1.8	0.2	0		0.7	0	0		3	0.7	0	25
enlarged	0.1	0.5	0.4		0.1	0.1	0		0.1	0.7	0.8	
irregular	0	0.3	0.4		0	0.2	0.2		0	0.1	0.8	
		pF %	3.9			pF %	1.4			pF %	6.2	
		p T %	8.1			p T %	9.2			p T %	10.4	
				round	0.1	0	0	95	0.9	0.1	0	65
				enlarged	0.1	0	0		0.1	0.2	0.1	
				irregular	0	0	0		0	0.1	0.1	
						pF %	0.2			pF %	1.6	
						p T %	8.7			p T %	8.3	
								round	1	0.4	0.1	120
								enlarged	0.1	0.3	0.2	
								irregular	0	0.1	0.8	
										pF %	3	
										p T %	12.2	

Site three shows an important porosity (2.2% in relation to the image total) constituted by big pores (T3) and small pores (T1); on the other hand, site two shows a reduced porosity (0.35%) with small and rounded pores (T1); site one shows an intermediate soil porosity (1.2%) with a small and big pore distribution.

An important increment of marked pores with blue of methylene was observed in site one (5.3 and 6.2%) with pores of all classes and shapes but with a trend to big and irregular pores.

The sedimentary transect (Table 7) shows functional porosity variation from 1.4 to 6.2% for surface horizons; on site 6 a functional porosity of 3.9% was observed with a trend of small and rounded pores (1.8%); site 5 shows a marked porosity of 1.4% of rounded and small pores (0.7%); likewise, site 4 shows a functional porosity higher (6.2%), here also preferential pores are small and rounded. These data allows a correlation of Ksat with porosity and calcareous accumulation.

Morphologic parameters of porosity and saturated hydraulic conductivity

Table 8 shows Ksat values and the parameters of total porosity (pt), functional porosity (pf) and the soil pore continuity index (*Ic*) for both transects. According the results, horizons with calcareous accumulation shows a Ksat values ranging from medium to low with correlation to *Ic* values close to zero and with a distribution of functional pores of small size and rounded shape.

Table 8. Morphological and hydrodynamic soil horizon characteristics.

Site	**depth cm**	**Ksat mm h^{-1}**	**pt %**	**Ic**	**pf %**
3	5	252	6	0.32	2.2
2	15	144	8	0.04	0.3
1	25	108	8	0.07	1.0
	95	108	10	0.10	5.4
	170	108	16	0.10	6.2
6	5	144	10	0.06	3.9
5	25	72	9	0.03	1.4
	95	108	9	0.04	0.2
4	25	108	11	0.1	6.2
	65	28.8	8	0.06	1.6
	130	32.4	12	0.11	3.05

Non calcareous horizons (riolite material) shows a higher Ksat with good continuity among pores as shown by *Ic* values with a morphologic distribution of functional pores of size ranging from medium to big and with enlarged and irregular shape with a less abundant distribution but with a higher participation on soil water dynamics when these are interconnected.

Conclusions

Soil water dynamics and void spaces correlations lead to mark preferential flow under saturated conditions in a watershed in northern Mexico and allowed to establish a morphological characterization of soil functional porosity using image analysis. This characterization according size, shape and pore continuity allowed to establish a typology of soil horizons with and without calcareous accumulation coherent with the hydrodynamic functionality.

When soil horizons shows calcareous formation, functional pores are small (< 0.53 mm^2) rounded and generally abundant. In this horizons soil water dynamics is a function of pore size and shape but mainly to the lack of connection among them.

In horizons without calcareous accumulation, functional pores are from medium (0.53 to 1.58 mm^2) to big (>1.58 mm^2) size with a spatial distribution less abundant than small pores. Nevertheless, in this horizons soil water dynamics depends on the type of shape of the pores (enlarged and irregular) and the continuity among them.

In general terms the horizons of the sedimentary transect showed values of Ksat lower than the eruptive transect due that the calcareous material is transported by water and deposited in the void spaces affecting soil pores continuity as shown by *Ic* values.

Comparison of total porosity values prevent to explain differences between Ksat; on the other hand, the continuity index and functional porosity allows to describe soil water dynamics for these horizons.

References

Beaudet, L. 1998. Organisation et fonctionnement hydrodynamique de mélanges limon argileux – tourbe blond. Essais mécaniques sous chargements répétés. Thèse de doctorat, Ecole Nationale Supérieure Agronomique de Rennes.

Bourier, J. 1965. Bulletin technique du Génie rural, No. 73. La mesure des caractéristiques hydrodynamique des sols par la méthode Vergière.

Bruand, A. 1986. Contribution à l'étude de la dynamique de l'espace poral. Utilisation des courbes de retrait et des courbes de rétention d'eau. Sci. Sol, 24:351-362.

Bullock, P., and J.A. McKeague. 1984. Estimating air-water properties of a clay soil. Comptes Rendus du colloque fonctionnement hydrique et comportement des sols, Dijon, 22-25 mai 1984, A.F.E.S., pp. 55-67.

Bouma, J., A. Jongerius, and D. Schoonderbeek, 1979. Calculation of saturated hydraulic conductivity of some pedal clay using micromorphometric data. Soil Science Society of America Journal 43:261-264.

Curmi P. 1988. Structure, espace poral du sol et fonctionnement hydrique. Analyse de quelques cas concrets. Sci. Sol, 26(3):203-214.

German, P., and K. Beven. 1981. Water flow in soil macropores. I. An experimental infiltration. Journal of Soil Science 32:1-13.

Grimaldi, M., and Bouler. 1989-90. Relation entre l'espace et le fonctionnement hydrodynamique d'une couverture pédologique sur socle de Guyane française. Cah. ORSTOM, sér. Pédologie., XXV(3):275-263.

González, C.G. 1998. Influences des practiques culturales sur la structure des couches supérieures de quatre vergers de noyer pecan (karya illinoensis, koch) irrigués de la Comarca Lagunera (Mexique). Diplome d'Etude Approfondi (DEA) National de Science du sol à Rennes France.

González, C.G. 2002. Fonctionnement hydrodynamique des sols de versant en amont de petits barrages en region semi-aride du Nord Mexique (Ranch Atotonilco). Thèse de doctorat, Université d'Angers, France.

Hallaire, V. 1997. Description of microcrack orientation in a clayey soil using image analysis. A.J. Ringrose-Voase and G.S. Humphreys, eds., Elseivier, Amsterdam.

Hallaire, V. and P. Curmi. 1994. Image analysis of pore space morphology in soil sections, in relation to water movement. In A.J. Ringrose-Voase and G.S. Humphreys, eds., Proceedings of Ninth International Working Meeting on Soil Micromorphology, pp. 559-567. Elsevier, Amsterdam.

Hallaire, V., P. Curmi, and Widiatmaka. 1997. Morphologie de la porosité et circulations préférentielles en saturé. Cas des horizons d'un système pédologique armoricain. Etude et Gestions des sols 4(2):115-126.

Murphy, C.P., P. Bullock, and R.H. Turner. 1977. The measurement and characterization of voids in soil thin sections by image analysis. Part I. Principles and techniques. Journal of Soil Science 28:498-518.

Serra J. 1982. Image Analysis and Mathematical Morphology. Academic Press, London.

Stengel P. 1979. Utilisation de l'analyse des systèmes de porosité pour la caractérisation de l'état physique du sol in situ. Ann. Agron. 30(1):27-51.